

AM4090 Write Up

Alison Pearn

January 2020

Abstract

Abstract will go here...

Contents

1	Introduction	3
1.1	Motivation	3
1.2	Reaction Advection-Diffusion Equations	4
1.3	The Equations	4
1.4	Model Simplification	7
1.5	Boundary Conditions	8
1.6	Variables of Interest	9
2	Method	10
2.1	Initial Approach	10
2.2	The Finite Difference Method	11
2.3	Discretising Boundary Conditions	11
2.4	Building Up to a Solution	13
2.5	Finding the Stationary Distribution	13
3	Results	16
3.1	Reproducing the Depth-Turbulence Plots	16
3.2	Stationary Distributions for Various Turbulence Values	18
3.3	Light Shifts	20
3.4	Study of a Particular Water Column	22
4	Discussion	26
4.1	Looking for Bifurcations	26

1 Introduction

1.1 Motivation

In the context of climate change and a growing human population, larger quantities of data than ever before, and powerful computers, ecological modelling and computer simulations are becoming increasingly important tools in the efforts to mitigate the effects of global warming, protect species from extinction and conserve the global food supply chain. Understanding and being able to form predictions about how ecological systems will react to shifts in the environment is essential for informing conservation policy in areas such as setting fishing quotas, establishing protected areas and choosing the least invasive strategies for developing agricultural landscape (11), (10). Also, if lacking a fundamental understanding of how ecosystems function, humans can unwittingly cause great damage to the natural world (16). With a global human population now predicted to reach 8.5 billion in 2030 (18), ensuring the persistence of food stocks is a major issue. As the climate becomes more volatile, the more understanding there is of the mechanisms behind ecological disasters such as pest-outbreaks, harmful algal blooms, and disease spreading (14) the better governing bodies will be able to prepare for the fallout of such events.

In the study of biodiversity it is often difficult and expensive to gather information about the distribution of various species, particularly in marine ecosystems (11)(16). Mathematical modelling offers a less expensive way to extrapolate what we do know about an ecological situation and draw useful conclusions.

Phytoplankton is an especially interesting topic of study due to its far-reaching influences. It is a significant primary producer and at the base of the aquatic food chain (9), so understanding the dynamics of phytoplankton populations can help form a basis for predictions about entire marine ecosystems (7). Phytoplankton blooms (red-tides) can lead to anaerobic conditions and dead zones (6) in the ocean or the release of toxins into the water (9) both which lead to the die-off of other marine life. Toxins released in harmful algal blooms (HABs) can also travel up the food-chain and affect human health (1). There has been considerable research into understanding the causes of red-tides but they are still not fully understood (16). Additionally, there is some scientific research going into the use of phytoplankton in bio-fuels (12),(4). All of this makes understanding the dynamics of phytoplankton populations especially topical and relevant and motivated it as the topic for this project. Models that allow scientists to understand what factors cause a population of phytoplankton to bloom or die-out are useful in evidence-based policy making.

1.2 Reaction Advection-Diffusion Equations

paragraph from introduction

Deterministic models, and in particular the branch of partial differential equations known as reaction advection-diffusion equations like those studied in this project are useful in many ecological situations. They are used to simplify the dynamics of an ecological system to its core elements and gain an understanding of the essential drivers of its evolution. In the case of population dynamics, a reaction advection-diffusion equation reduces the complex list of factors which affect some population to its patch size, production rate, death rate, and rates of spreading (advection and diffusion). Obviously this is a drastic oversimplification and insufficient to describe any real-life situation, however it can be useful in a number of ways. Simple models can capture some of the fundamental mechanisms of a population's behaviour and allow us to gain a basic intuition for the relationship between various factors which can then be built upon. Also, if there exist clear reasons for the occurrence of a certain phenomenon then it may also be applicable in the real world. Though most classical bifurcations in dynamical systems become degenerate with even small perturbations, saddle-node bifurcations and tipping points do exist in nature (16) and simplified models can help scientists understand at what values they may occur and even form a basis for scientific predictions of the effects of environmental changes on biodiversity and populations of species.

1.3 The Equations

This project studies a deterministic model proposed by Jäger, C., Diehl, S. and Emans, M. (8), which consists of a set of three coupled nonlinear partial differential equations and two differential equations that describe the vertical dynamics of phytoplankton in a one-dimensional column of freshwater. For this model, the z-axis is inverted and deeper depths correspond to greater z-values. The equations are as follows (8),

$$\frac{\partial A}{\partial t} = p(I, q)A - l_{bg}A - v \frac{\partial A}{\partial z} + d \frac{\partial^2 A}{\partial z^2} \quad (1a)$$

$$\frac{\partial R_b}{\partial t} = \rho(q, R_d)A - l_{bg}R_b - v \frac{\partial R_b}{\partial z} + d \frac{\partial^2 R_b}{\partial z^2} \quad (1b)$$

$$\frac{\partial R_d}{\partial t} = -\rho(q, R_d)A + l_{bg}R_b + d \frac{\partial^2 R_d}{\partial z^2} \quad (1c)$$

$$I(z) = I_0 \exp - \left(\int_0^z kAdz + k_{bg}z \right) \quad (1d)$$

$$\frac{\partial R_s}{\partial t} = vR_b(z_{max}) - rR_s \quad (1e)$$

with functions p and ρ ,

$$p(I, q) = \mu_{max} \left(\frac{q - q_{min}}{q} \right) \frac{I}{h + I} \quad (2a)$$

$$\rho(q, R_d) = \rho_{max} \left(\frac{q_{max} - q}{q_{max} - q_{min}} \right) \frac{R_d}{m + R_d} \quad (2b)$$

and,

$$q = \frac{R_b}{A} \quad (3)$$

Phytoplankton are photosynthesising organisms, they grow best in well-lit conditions with plenty of available nutrients (phosphorus in this case). At all depths algae will take in dissolved nutrients at a rate ρ , dependant on how many dissolved nutrients are available at that depth, $R_d(z)$, and how “well-fed” the algae already are. Once taken in, these nutrients are bound to the algae and hence they will move with identical dynamics. How “well-fed” algae are at a certain depth can be quantified by the ratio, q , between the concentrations of bound nutrients, R_b , and algae, A , present. In marine ecosystems, the euphotic zone is the shallow top layer of water where it is sufficiently bright to allow for photosynthesis (5). The growth of algae is hence limited to shallower water. The phytoplankton in this model are suspended in the water and not free-swimming so will sink helplessly out of the euphotic zone under the force of gravity at a rate v . They can only be transported back into this zone via the turbulence in the water, which is diffusing at a rate of d at all depths. This makes turbulence a significant factor in the dynamics of algal populations.

The equations here show algae and bound nutrients drifting and diffusing vertically in a one-dimensional column of water. The algal population grows with the photosynthesis-representing source term $p(I, q)$ and declines at a constant rate of respiration l_{bg} , which behaves as a sink term. It is assumed that the system is closed for nutrients R , which can exist in three states: bound to the algae, dissolved in the water and sedimented as R_s at z_{max} , the bottom of the water column. The state of these nutrients evolves in a cyclical fashion. Algae takes up dissolved nutrients from the water at a rate ρ , changing R_d to R_b . When algae reach z_{max} it is assumed that the algae simply die, disappear from the system and their nutrients become sedimented as R_s . These sedimented nutrients then dissolve back into the water as R_d again at a rate r .

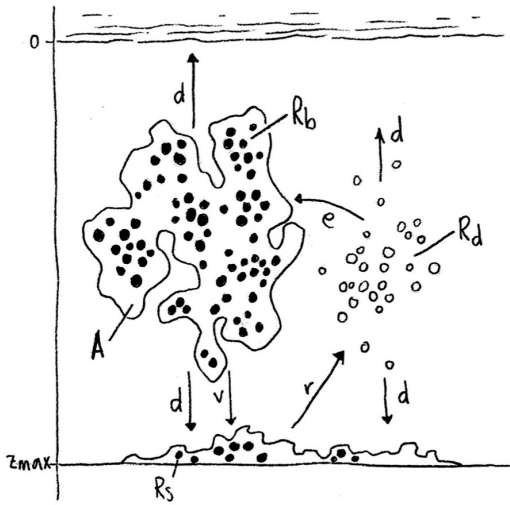


Figure 1: Phytoplankton take in dissolved nutrients (white dots) at a rate ρ , converting them to particulate nutrients (black dots) bound in the phytoplankton. The bound nutrients diffuse up and down at a rate d and sink at a rate v with the phytoplankton cloud. When bound nutrients reach z_{max} they become sedimented as R_s . Sedimented nutrients are released back into the water column as dissolved nutrients at a rate r . The dissolved nutrients also diffuse up and down at a rate d but do not sink.

The actual depth of the euphotic zone will depend on the concentration of phytoplankton present. Light intensity I will always decrease with depth as light is attenuated by background particles in the water at a rate k_{bg} but algae will also attenuate light at a rate k . Hence if there is a high concentration of algae at the surface it may be reasonable to assume that the euphotic zone will be slightly shallower in the water.

limited to slightly shallower water

Variable	Value	Definition
A		algal carbon density ($\text{mg } C \text{ m}^{-3}$)
R_b		Concentration of particulate nutrients bound in algae ($\text{mg } P \text{ m}^{-3}$)
R_d		Concentration of dissolved nutrients ($\text{mg } P \text{ m}^{-3}$)
R_s		Pool of sedimented nutrients ($\text{mg } P \text{ m}^{-2}$)
I		Light intensity ($\mu\text{mol photons m}^{-2} \text{ s}^{-1}$)
I_0	300	Light intensity at the surface ($\mu\text{mol photons m}^{-2} \text{ s}^{-1}$)
d	0.01-1000	Turbulent-diffusion coefficient ($\text{m}^2 \text{ day}^{-1}$)
v	0.25	Algal sinking velocity (m day^{-1})
l_{bg}	0.1	Specific algal maintenance respiration losses (day^{-1})
k	.0003	Specific light-attenuation coefficient of algal biomass ($\text{m}^2 \text{ mg } C^{-1}$)
k_{bg}	0.4	Background light-attenuation coefficient (m^{-11})
μ_{max}	1.2	Maximum specific algal production rate (day^{-1})
q_{min}	0.004	Maximum algal nutrient quota ($\text{mg } P \text{ mg } C^{-1}$)
q_{max}	0.04	Minimum algal nutrient quota ($\text{mg } P \text{ mg } C^{-1}$)
h	120	Half-saturation constant of light-dependant algal production ($\mu\text{mol photons m}^{-2} \text{ s}^{-1}$)
ρ_{max}	0.2	Maximum specific algal nutrient uptake rate ($\text{mg } P \text{ mg } C^{-1} \text{ day}^{-1}$)
m	1.5	Half-saturation constant of algal nutrient uptake ($\text{mg } P \text{ m}^{-3}$)
r	.02	Specific mineralisation rate of sedimented nutrients (day^{-1})

Table 1: Table of variables used, taken from Jäger et al. (8)

1.4 Model Simplification

The model in (8) is of course a huge simplification of the true dynamics of phytoplankton in an aquatic environment. It is assumed that the only direct limiting factors to algal growth are light and phosphorus availability. Algae and a single nutrient are isolated from all other elements of a marine ecosystem such as alternative nutrients like nitrogen (REF), predators, and other organisms competing for nutrients with the algae. Light intensity is uniform and not adjusted to reflect day and night or seasons and diffusion and sinking coefficients are not only constant in time but also in depth. This is unrealistic as it does not account for the increased turbulence that occurs near the surface of bodies of water (REF). The model is 1-dimensional so changing depths on the lake floor are not accounted for and this may have considerable impact on the behaviour of the system.

Nonetheless, this model can educate us on the basic behaviour of algae and form a blueprint for further study upon which more models that account for more of the ecosystem's true complexity can be built. There is a possibility that mechanisms discovered in this simple model will translate

and still be relevant in more complex models and perhaps uncover fundamental truths about the drivers of a population of phytoplankton's dynamics.

1.5 Boundary Conditions

The same boundary conditions as provided in the paper (8) are used in this project and these are shown in table 2 below.

Algae, particulate and bound nutrients can neither enter nor leave the water column at the surface. To establish this, Robin and Neumann boundary conditions are set such as the convective flux for all three variables is zero. As the dynamics of A and R_b are governed by both drift and diffusion and those of R_d by diffusion alone, their net currents can be described as,

$$\begin{aligned} J_A &= vA - dA' \\ J_{R_b} &= vR_b - dR'_b \\ J_{R_d} &= -dR'_d. \end{aligned}$$

Setting J_A , J_{R_b} and J_{R_d} to zero at the surface yields the boundary conditions provided in table 2.

When algae reach z_{max} they are assumed to sink out of the system, the particulate nutrients which are bound to them then become part of the sediment R_s . This means that at $z = z_{max}$ there is no diffusion of algae and bound nutrients and their net current is a downward drifting current only, i.e. only the drift current may contribute to the settling of particulate nutrients at z_{max} . To achieve this, Neumann boundary conditions are used which set the diffusive element of the current dA' , dR'_b to zero, giving rise to the conditions in table 2. The Robin boundary condition for R_s and R_d then preserves the concentration of nutrients in the system by ensuring the influx current of nutrients into R_s from R_d via diffusion d is equal to the outflux by remineralisation r , $J_{R_d} = -dR'_d = -rR_s$.

Neumann conditions at $z = 0$ and $z = z_{max}$ also indicate that minima and maxima must occur for A and R_b at z_{max} and for R_d at the surface. This can be seen relatively clearly in figure 6 for turbulence values $d = 0.1, 1.0$ where the z_{max} shifts from behaving as a maximum in shallow water columns, to behaving as a minimum in deeper water columns. This is less clear for water with turbulence $d = 100$ so it is illustrated in the appendix in figure A2 where the line plots are all achieving minima at z_{max} for A , maxima at z_{max} for R_b and minima at 0 for R_d . **Note:** If the sediment layer is kept constant at zero then $vR_b = rR_s$ leading to the boundary condition in column z_{max} (i), allowing us to perform calculations without R_s .

Variable	Surface	z_{max} (i)	z_{max} (ii)
A	$vA(0) - dA'(0) = 0$	$A'(z_{max}) = 0$	$A'(z_{max}) = 0$
R_b	$vR_b(0) - dR'_b(0) = 0$	$R'_b(z_{max}) = 0$	$R'_b(z_{max}) = 0$
R_d	$R'_d(0) = 0$	$dR'_d(z_{max}) - vR_b(z_{max}) = 0$	
I	$I(0) = I_0$		$rR_s - dR'_d(z_{max}) = 0$

Table 2: Boundary conditions, taken from Jäger et al. (8)

1.6 Variables of Interest

plenty of for

There were numerous potential areas of exploration in this model, the ratio between the total amount of nutrients in the system (DISCUSSION)

As light is needed for algal growth, the majority of production will occur in the euphotic zone of the water column, where $I(z)$ is large. As the algae in this model do not have the ability of self-propulsion and have a higher density than water they will sink out of this zone at a rate v , along with the nutrients that are bound to them. Only turbulence can transport them back into a depth where production can take place, otherwise they will die out at a rate $k_{bg}A$ near z_{max} where it is very dark and photosynthesis cannot occur, or enter the sediment and disappear from the system (8).

The variables of focus chosen for this project are d , the degree of turbulence in the water, and I_0 the light intensity at the surface and the intention is to develop a thorough understanding of the mechanism by which these variables will affect the rest of the system.

This project aims to reproduce the results of Jäger et al. (8) in the water column depth-turbulence space and examine changes caused by shifts in d and I_0 .

There are plenty of potential areas for exploration in this model. The total amount of nutrients in the system would inform at which levels we can expect eutrophication and algal blooms to occur and for what duration. We could explore how murkier water affected population survival by increasing the background light attenuation coefficient of the water k_{bg} or explore how the model changes for algae with a higher density by increasing their sinking rate v .

One of the most interesting variables in the model is the turbulence d because, unlike water clarity (which we expect to improve algal survival rates) and sinking velocity v (which we expect to decrease survival rates as algae become lost in the sediment more rapidly) the effect of d is not immediately clear.

2 Method

2.1 Initial Approach

To find equilibrium solutions for the system the initial approach used set all partial time derivatives to zero and attempted to solve the new system of ordinary differential equations. This was attempted via the shooting method. By defining $A_2 = A'$, $R_{b2} = R'_b$ and $R_{d2} = R'_d$ as new variables with $A' = \frac{\partial A}{\partial z}$, the system was reduced to the first-order system given below,

$$\begin{aligned} A'_1 &= A_2 \\ A'_2 &= \frac{1}{d}(vA_2 - p(I, q)A_1 + l_{bg}A_1) \\ R'_{b1} &= R_{b2} \\ R'_{b2} &= \frac{1}{d}(vR_{b2} - \rho(q, R_{d1})A_1 + l_{bg}R_{b1}) \\ R'_{d1} &= R_{d2} \\ R'_{d2} &= \frac{1}{d}(\rho(q, R_{d1})A_1 - l_{bg}R_{b1}) \\ I' &= -(kA_1 + k_{bg}z)I \end{aligned}$$

with boundary conditions,

$$\begin{aligned} vA_1(0) - dA_2(0) &= 0 & A_2(z_{max}) &= 0 \\ vR_{b1}(0) - dR_{b2}(0) &= 0 & R_{b2}(z_{max}) &= 0 \\ R_{d2}(0) &= 0 & dR_{d2}(z_{max}) - vR_{b1}(z_{max}) &= 0 \\ I(0) &= I_0 & & \end{aligned}$$

ref

Taking the initial homogeneous conditions for $A_1 = 300$, $R_{b1} = 2.2$, $R_d = 30$ and $I = 300$ as known, the remaining values for A_2 , R_{b2} and R_{d2} were guessed and a fourth-order Runge-Kutta method was used to interpolate the initial value problem to z_{max} . The predicted values for A_2 , R_{b2} and R_{d2} and $dR_{d2} - vR_{b1}$ would be compared to the given boundary conditions. The intention was to then treat the differences between predicted and given boundary conditions as an equation in $A_2(0)$, $R_{b2}(0)$ and $R_{d2}(0)$ and solve for its roots by the multivariate Newton-Raphson method. (REF) [scipy.optimize.root & REF](#)

The values at z_{max} obtained via Runge-Kutta iteration displayed very high sensitivity to initial conditions and the majority of chosen initial conditions led to the solution blowing up. Hence any shooting method implementations failed to converge. This suggested that the system may be a stiff system (3), so instead a finite difference method was used to calculate the solutions for subsequent time steps over a long period of time until the system began to settle into a stable, stationary distribution.

*To allow for this possibility a different approach was taken:
the finite difference method...*

To achieve the results shown in the rest of this project,

2.2 The Finite Difference Method

An explicit finite difference method was used to obtain numerical approximations of the differential equations 1a-1e. The first-order time derivative was approximated by the forward Euler method and the first and second-order space derivatives were approximated by first and second-order central difference equations. This yielded,

$$A_z^{t+\Delta t} = A_z^t + \Delta t \left(p(I_z^t, q_z^t) A_z^t - l_{bg} A_z^t - v \frac{A_{z+\Delta z}^t - A_{z-\Delta z}^t}{2\Delta z} + d \frac{A_{z+\Delta z}^t - 2A_z^t + A_{z-\Delta z}^t}{\Delta z^2} \right) \quad (4)$$

$$R_{bz}^{t+\Delta t} = R_{bz}^t + \Delta t \left(\rho(q_z^t, R_{dz}^t) A_z^t - l_{bg} R_{bz}^t - v \frac{R_{bz+\Delta z}^t - R_{bz-\Delta z}^t}{2\Delta z} + d \frac{R_{bz+\Delta z}^t - 2R_{bz}^t + R_{bz-\Delta z}^t}{\Delta z^2} \right) \quad (5)$$

$$R_{dz}^{t+\Delta t} = R_{dz}^t + \Delta t \left(-\rho(q_z^t, R_{dz}^t) A_z^t + l_{bg} R_{bz}^t + d \frac{R_{dz+\Delta z}^t - 2R_{dz}^t + R_{dz-\Delta z}^t}{\Delta z^2} \right) \quad (6)$$

$$R_s^{t+\Delta t} = R_s^t + \Delta t (v R_{bz_{max}}^t - r R_s^t) \quad (7)$$

and equation 1d for I is discretized by expressing $\int_0^z kAdz$ as $\sum_i kA(i)\Delta z$ where $i = 0, \Delta z, 2\Delta z, \dots, z$.
then

2.3 Discretising Boundary Conditions

To discretise the boundary conditions in table 2 the second-order formula for the first derivative (15), $f'(x) = \frac{1}{2h} (-3f(x) + 4f(x+h) - f(x+2h)) + O(h^2)$ is used.

In the case of Neumann boundaries where $f'(x) = 0$ this simplifies to,

$$\begin{aligned} -3f(0) + 4f(1) - f(2) &= 0 \\ -f(M-2) + 4f(M-1) - 3f(M) &= 0 \end{aligned}$$

which give us,

$$R_{d0} = \frac{1}{3}(4R_{d1} - R_{d2})$$

for the boundary condition for R_d at the surface. To obtain a second order discretisation of the Robin boundary conditions at the surface,

$$\begin{aligned} 0 &= vA_0 - \frac{d}{2\Delta z} (-3A_0 + 4A_1 - A_2) \\ \implies A_0 &= \frac{d}{2v\Delta z + 3d} (4A_1 - A_2) \end{aligned}$$

and,

$$R_{b0} = \frac{d}{2v\Delta z + 3d} (4R_{b1} - R_{b2})$$

and similarly at z_{max} with $M = z_{max}$,

$$\begin{aligned} A_M &= \frac{1}{3}(-A_{M-2} + 4A_{M-1}) \\ R_{bM} &= \frac{1}{3}(-R_{bM-2} + 4R_{bM-1}). \end{aligned}$$

For the Robin condition,

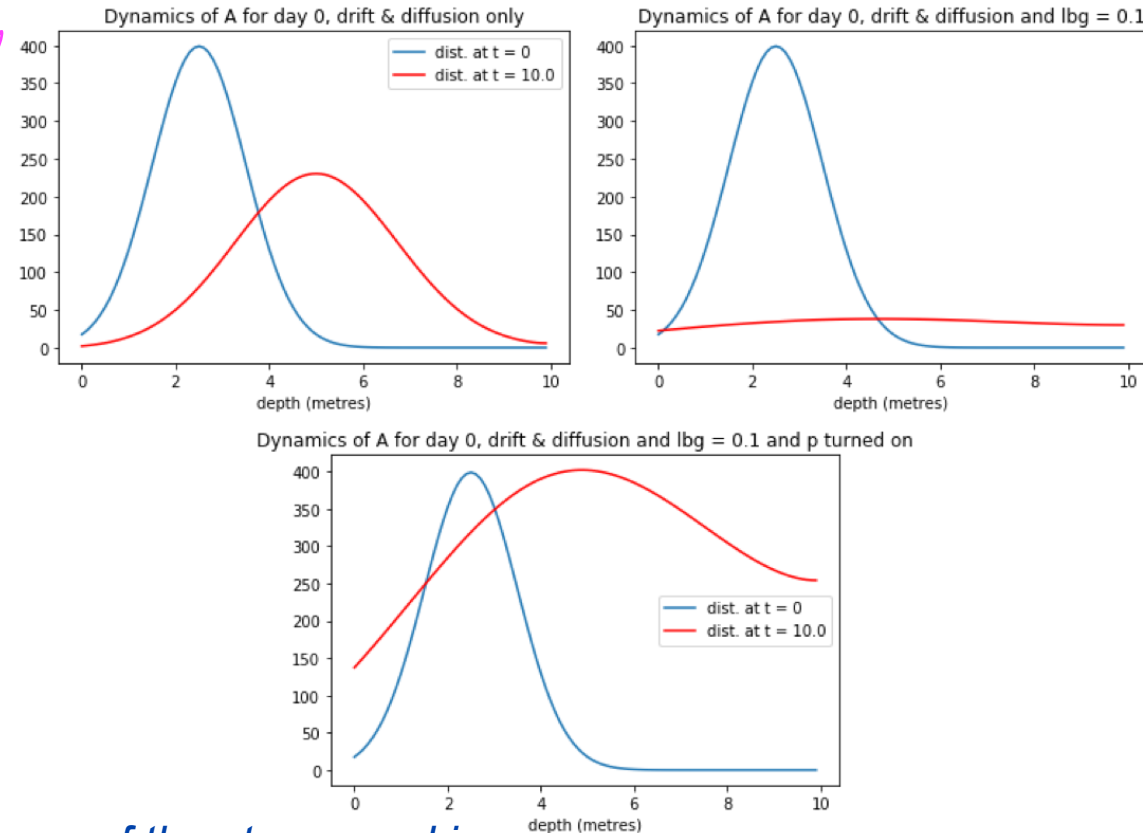
$$\begin{aligned} 0 &= rR_{sM} - \left(-\frac{d}{2\Delta z} (-3R_{dM} + 4R_{dM-1} - 3R_{dM-2}) \right) \\ \implies R_{dM} &= \frac{1}{3d} (4dR_{dM-1} - dR_{dM-2} + 2r\Delta z R_{sM}). \end{aligned}$$

These results are summarised in table 3.

Variable	Surface	z_{max}
A	$A_0 = \frac{d}{2v\Delta z + 3d} (4A_1 - A_2)$	$A_M = \frac{1}{3}(-A_{M-2} + 4A_{M-1})$
R_b	$R_{b0} = \frac{d}{2v\Delta z + 3d} (4R_{b1} - R_{b2})$	$R_{bM} = \frac{1}{3}(-R_{bM-2} + 4R_{bM-1})$
R_d	$R_{d0} = \frac{1}{3}(4R_{d1} - R_{d2})$	$R_{dM} = \frac{1}{3d} (4dR_{dM-1} - dR_{dM-2} + 2r\Delta z R_{sM})$
I	$I(0) = I_0$	

Table 3: Discretised boundary conditions

2.4 Building Up to a Solution



some of the steps used in ref. equations

Figure 2: Figure showing steps to build up to the full model. First a model of just drift and diffusion was created, then the loss term l_{bg} was added, followed by the production term p in a step-by-step fashion

The final solution was built up to in a series of steps in order to make sure everything was working as

expected three

It should be. Three diagrams showing some of these steps are shown in figure 2. First the equations for A were simplified to drift-diffusion only equations and these were approximated by the finite difference method. An initial concentration with a 'bump' a quarter of the way down the water column was considered and this bump can be seen sinking down the water column and diffusing out.

When the l_{bg} -term was added this bump shrinks dramatically and the overall concentration of A is reduced. When the p function is finally included the concentration increases. The effect of these terms can be emphasised by tweaking v, d and l_{bg} accordingly.

2.5 Finding the Stationary Distribution

dist of the conc of

To find the stationary concentration distributions of phytoplankton and nutrients in the water column the finite difference method was used to calculate consecutive steps until the solution stopped

system

changing with time. The time at which the solution settled into a stationary distribution varied depending on the values of turbulence d and water column depth z_{max} . This was easiest to visualize using 3-dimensional surface plots. Figure 3 shows that for $d = 0.1$ and $z_{max} = 30$ the solution doesn't reach its stationary distribution until around 800 days but in figure 4 the solution with $d = 10$ and $z_{max} = 10$ settles in under 200 days. For low values of d like in figure 3 the solution oscillated around its stationary distribution before it settled into it and this behaviour was more exaggerated with deeper water column depths. More examples of these time-evolution plots are given in figure A1 in the appendix. Table 4 shows how long it took solutions to settle into a stationary distribution for different combinations of (z_{max}, d) -pairs.

	$z_{max} = 10$	$z_{max} = 30$
$d = 0.1$	400	> 800
$d = 1$	< 200	< 300
$d = 10$	< 200	< 200
$d = 100$	200	300

Table 4: The number of days before solution became stationary for (d, z_{max}) -pairs.

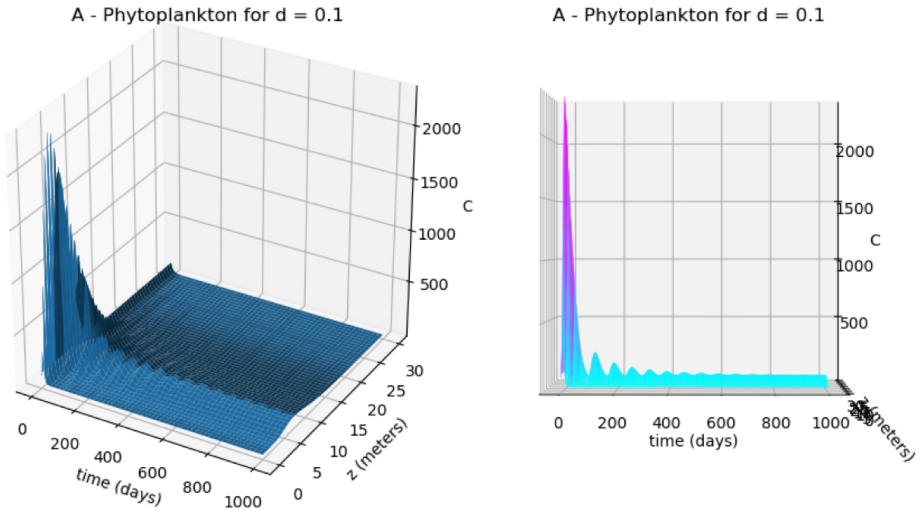


Figure 3: Surface plots showing the evolution of phytoplankton concentrations over time for $z_{max} = 30$ and $d = 0.1$. The system reaches a stationary distribution around day 800.

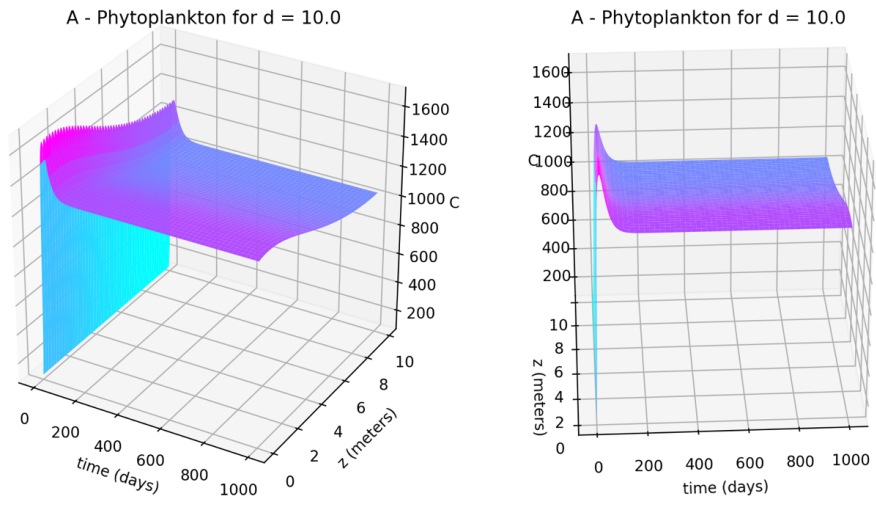


Figure 4: Surface plots showing the evolution of phytoplankton concentrations over time for $z_{max} = 10$ and $d = 10.0$. The system reaches its stationary distribution before day 200.

3 Results

3.1 Reproducing the Depth-Turbulence Plots

The first aim of this project was to reproduce the heatmaps of the first two rows of figure 5 which was taken from the paper by Jäger et al. (8). The first row here shows concentrations of phytoplankton at different depths z (z -axis), for different water column depths z_{max} (x -axis), for five different turbulence values $d = \{0.1, 1, 10, 100, 1000\}$. The second row shows the same for total nutrient concentration $R = R_d + R_b$. Being able to reproduce these heatmaps would both verify the accuracy of (8) and ensure the finite difference method used here is calculated correctly and that any conclusions drawn from it's implementation are reliable.

As this method was quite computationally intensive a step size of $\Delta z = 0.1$ with a corresponding time step of $\Delta t = \frac{\Delta z}{1000}$ was chosen instead of $\Delta z = 0.02$ as in (8). Stationary distributions were calculated thirty times for water columns of depth $0 - 30$ instead of $0 - 50$ and this is taken as sufficient to conclude that the approximations agree. The value of $d = 1000$ was omitted also omitted. For $d = 100$ a smaller timestep ratio of $\Delta t = \frac{\Delta z}{2000}$ was required (SAY WHY) and a corresponding slightly larger spacial step $\Delta z = 0.2$ was used in order to keep the simulation running reasonably fast.

The number of finite difference steps needed to reach a stationary distribution varied for each value of d and these figures are shown in days in table 4. For each d value the simulation was run for the number of days needed for the $z_{max} = 30$ water column to reach a stationary distribution. In the case of $d = 0.1$ the simulation was only run until day 600 in order to save time, it can be seen in figure 3 that this is still reasonably close to the true stationary distribution of A .

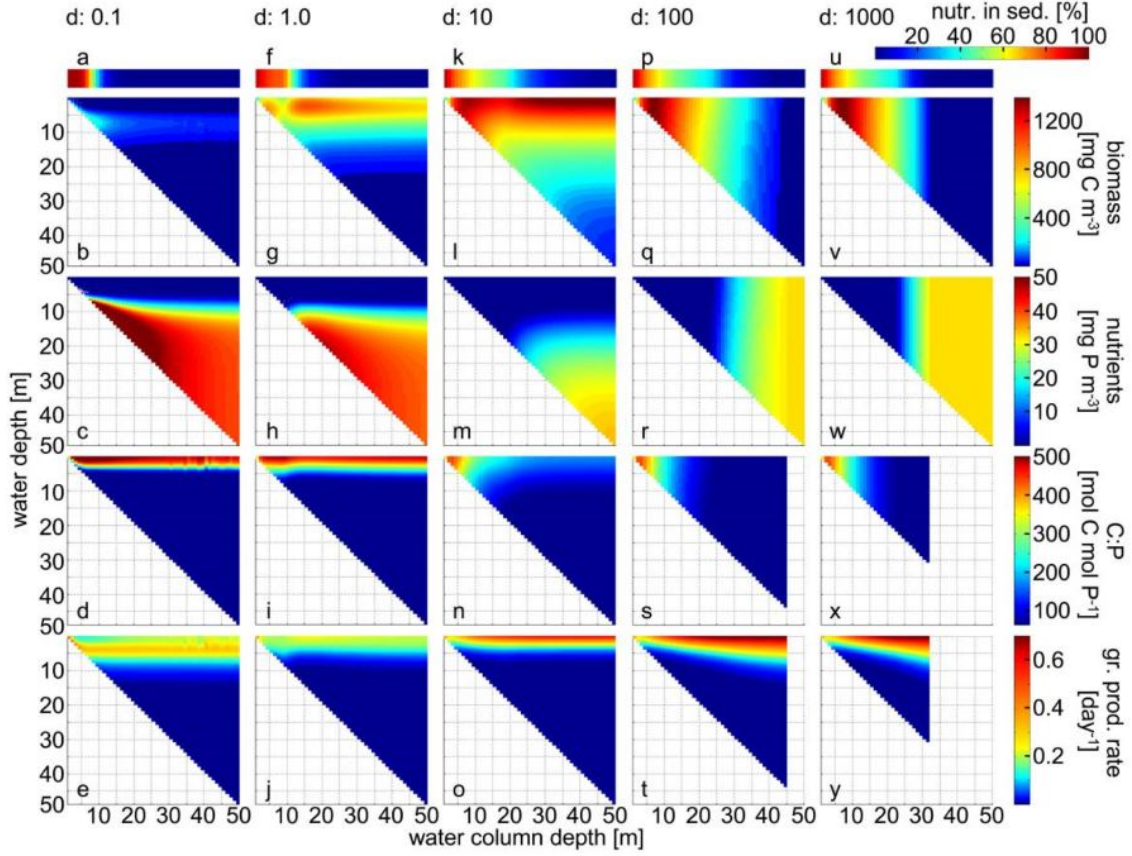


Figure 5: Stationary distributions of phytoplankton and nutrient concentrations for different turbulence values in the water column depth-depth space, from Jäger et al. (8)

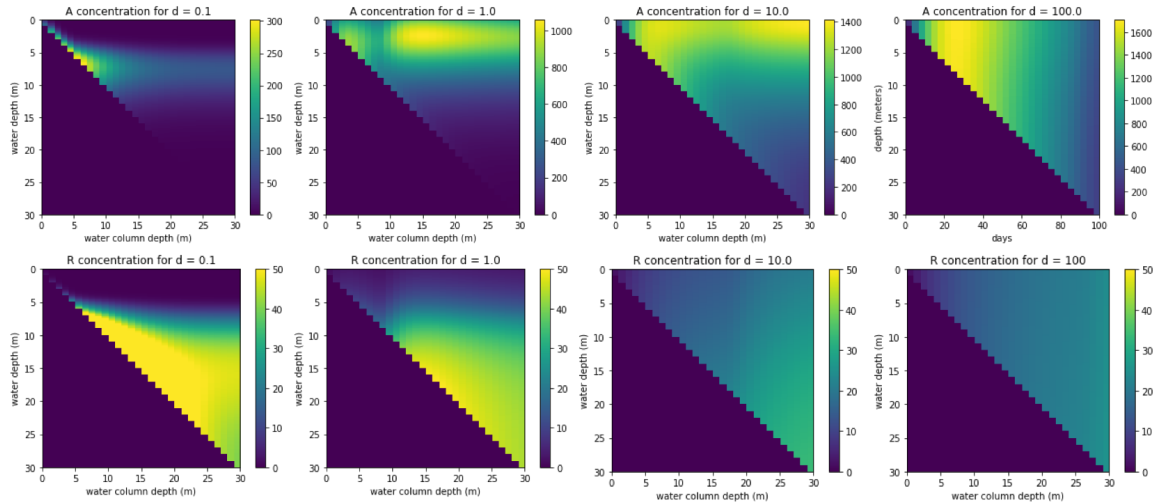


Figure 6: *Stationary distributions of phytoplankton and nutrient concentrations for different turbulence values in the water column depth-depth space approximated by the finite difference method*

3.2 Stationary Distributions for Various Turbulence Values

A plot of the stationary distribution changing with d for a fixed water column depth is useful to get a clearer idea of how changes in d alone affect algal distributions. Figures 7 and 8 show the stationary distributions of A and R_b for values of d ranging from 0 – 10. Very small values of d , in the range 0 – 0.5 do not appear sufficient to sustain an algal population for a water column of depth 15 metres, suggesting that there is not enough turbulence bringing algae back into the euphotic zone to sustain life. The distribution of A and R_b show pronounced peaks between $d = 2$ and $d = 4$ which hint that the depth of optimal conditions and maximum production lies between these two peaks. These peaks then soften as d increases past 6 and the noise from the turbulence slightly obscures information about where production is occurring.

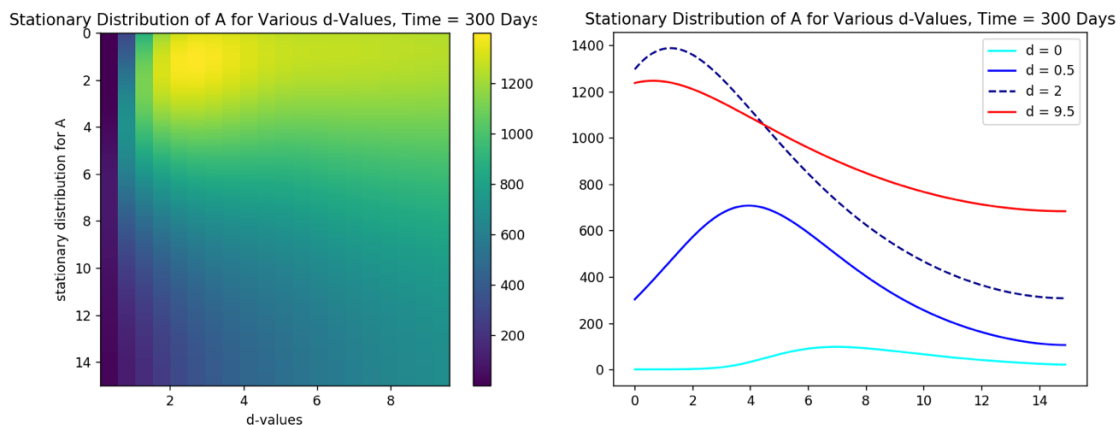


Figure 7: *Stationary distributions of A for $d \in [0, 10]$*

*In order to obtain a clearer picture
of how changes in d ... a plot of...
is useful*

*all the notes from copy book
put in here!*

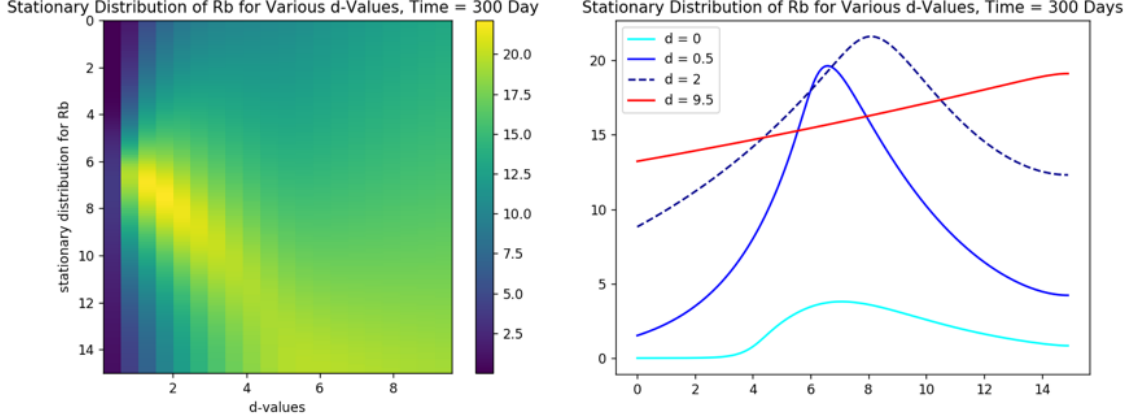


Figure 8: *Stationary distributions of R_b for $d \in [0, 10]$*

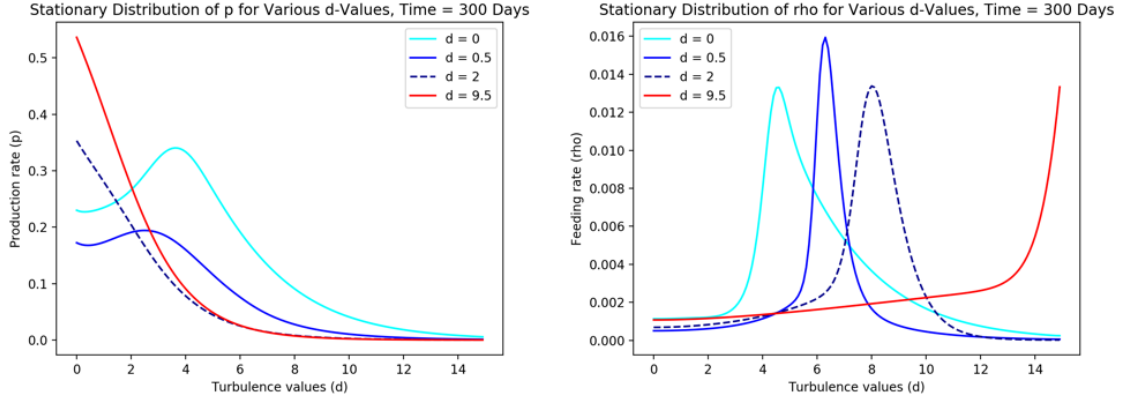


Figure 9: *The distributions of the production rate p and nutrient uptake rate ρ .*

Figure 9 shows the distribution of p the production rate and ρ the nutrient uptake rate for d -values of $\{0, 0.5, 2, 9.5\}$ and figure 10 shows the same for light intensity and algal nutrient quota. For $d = 9.5$ the majority of nutrient uptake ρ happens near the bottom of the water column but the turbulence quickly redistributes algae throughout the water column so can well-fed algae can photosynthesise near the surface. This creates good conditions for a high, evenly distributed algal population as all algae in the system are involved in production.

Contrastingly, when turbulence is low, as in the light blue line, algae (WHY DOES RHO MOVE DOWN WITH THE TUBRULENCE???)

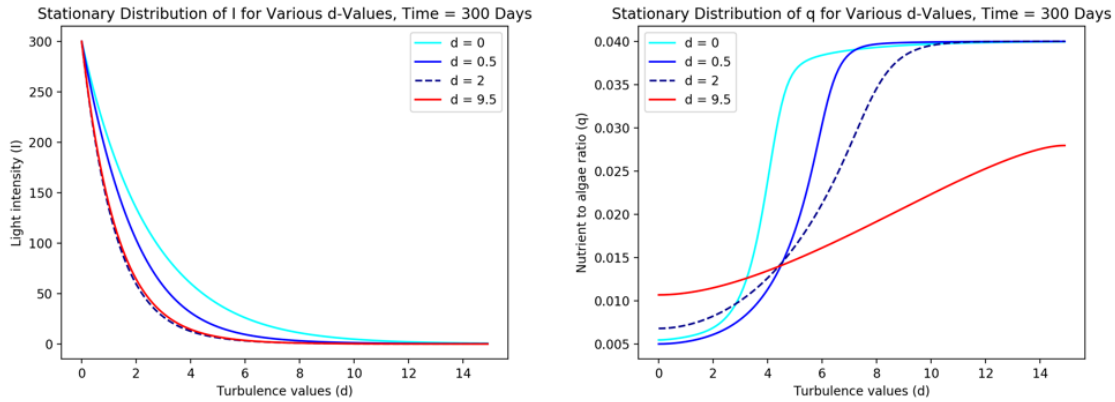


Figure 10: *The distributions of light intensity I and algal nutrient quota q .*

3.3 Light Shifts

the impacts of light intensity on this model

To explore how changes in light intensity affect the dynamics of phytoplankton populations a number of simulations were run on a water column of depth $z_{max} = 30$. In the heatmap on the left of figure 11 the light intensity at the surface was doubled to $600 \mu mol photons m^{-2} s^{-1}$ at $t = 60$ days and the solution quickly moves to a new stationary distribution of almost double the concentration. The heatmap in figure 11 shows an arcing front as phytoplankton at the surface are affected first and this change then spreads to deeper depths over time. The right-hand heatmap of figure 11 displays the an almost equal and opposite effect when the light intensity at the surface was halved to $150 \mu mol photons m^{-2} s^{-1}$.

arcing fronts
the hmap on the right-hand side

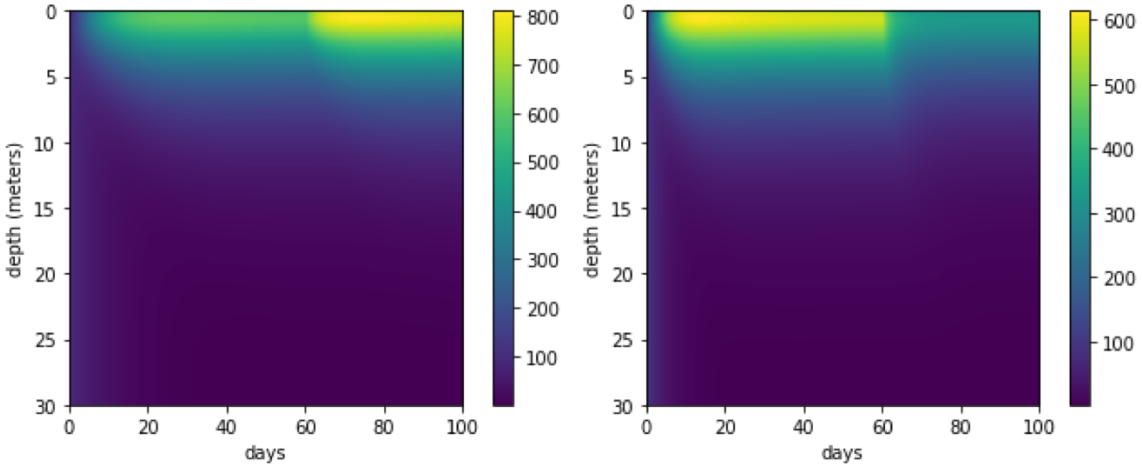


Figure 11: The heatmap of the left shows the effect of light intensity doubling from 300 to 600 on the 60th day. The heatmap on the right shows the effect of light intensity being halved on day 60.

Next, the scenario of a period of total darkness, where there was no light at all for a number of days, was considered. The intention was to see how the phytoplankton populations would react and if, and how quickly, they would recover. This would be applicable in situations of an extreme climate event, such as a Tambora volcanic eruption in 1815 where a distance of 600km was thrown into darkness for two days (17) or in an oil spill, where the surface of the sea in any areas of water coated in oil would obviously be obscured from sunlight.

Simulations were run for various turbulence levels over 500 days on water columns of depth 20m and a 10 day period of darkness occurred on the 250th day. Figure 12 shows results for $d = 5$. Figures for $d = 1, 10$ and 100 can be seen in the appendix, figures A3, A4 and A5 . These figures show concentrations recover quickly from periods without light and even increase a little beyond the stationary distribution for a short time before settling back to original values.

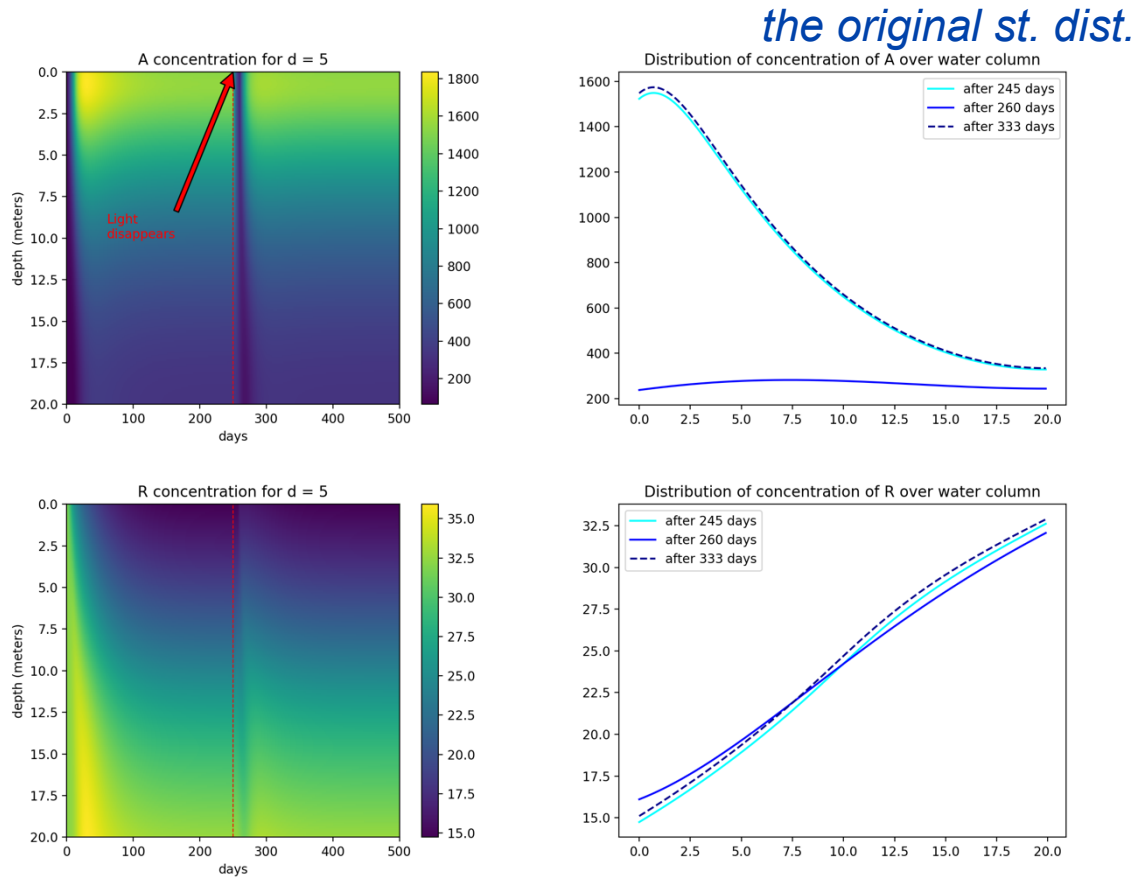


Figure 12: Light disappears for 10 days on the 250th day, indicated by the red dashed line. Conditions are $d=5$, $z_{max}=20m$. Algal populations drop to a lower, more homogeneous distribution of $A \approx 200$ while light is absent but make a full recovery within 100 days of light returning. In fact, the population **slightly** **surpasses the** stationary distribution for a brief period of time after the light returns.

mg P m⁻³

3.4 Study of a Particular Water Column

Special attention was given to the water column with $d = 1.0$ and depth $z_{max} = 20$ because, as can be seen in figure 6: the phytoplankton **displays** had an interesting nontrivial peak in its stationary distribution for this (d, z_{max}) -pair. The simulation was run for 1000 days to ensure there was sufficient time for a stationary distribution to be reached before and after the light disappearance, which lasted for 100 days on the 500th day. Heatmaps of the phytoplankton and nutrient distributions over the 1000 days are shown in figure 13. The mechanics by which the population originally grows become more apparent in figure 14 which enlarges the first 100 days in the water column. Nutrients initially have a homogeneous distribution throughout the water and phytoplankton populations bloom due to the high availability of nutrients in the euphotic zone. However as nutrients become bound in the algae they sink with it and by day 18 the bulk of the nutrients are gathered around 7m below the surface. This peak concentration of nutrients moves slowly down until the distribution in R -concentration resembles a smooth positive gradient from 0 to z_{max} . This **behaviour acts as** as a natural brake on phytoplankton blooms near the surface.

this process behaves as a

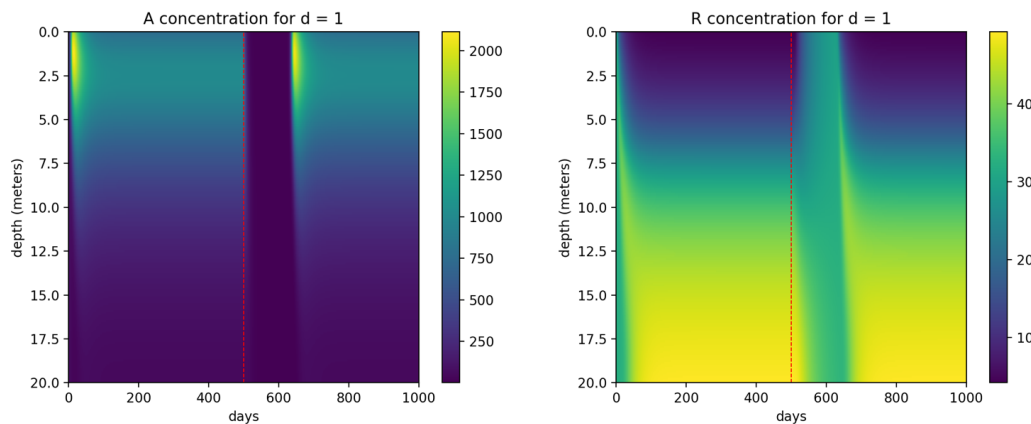


Figure 13: Heatmaps showing the evolution of phytoplankton and nutrient distributions with time. Light disappears for 100 days on the 500th day, marked with a red dashed line

In order to gain a more thorough understanding of the mechanisms by which phytoplankton populations respond to light changes, the water column with...is given special attention. This column is interesting because the plankton displays...

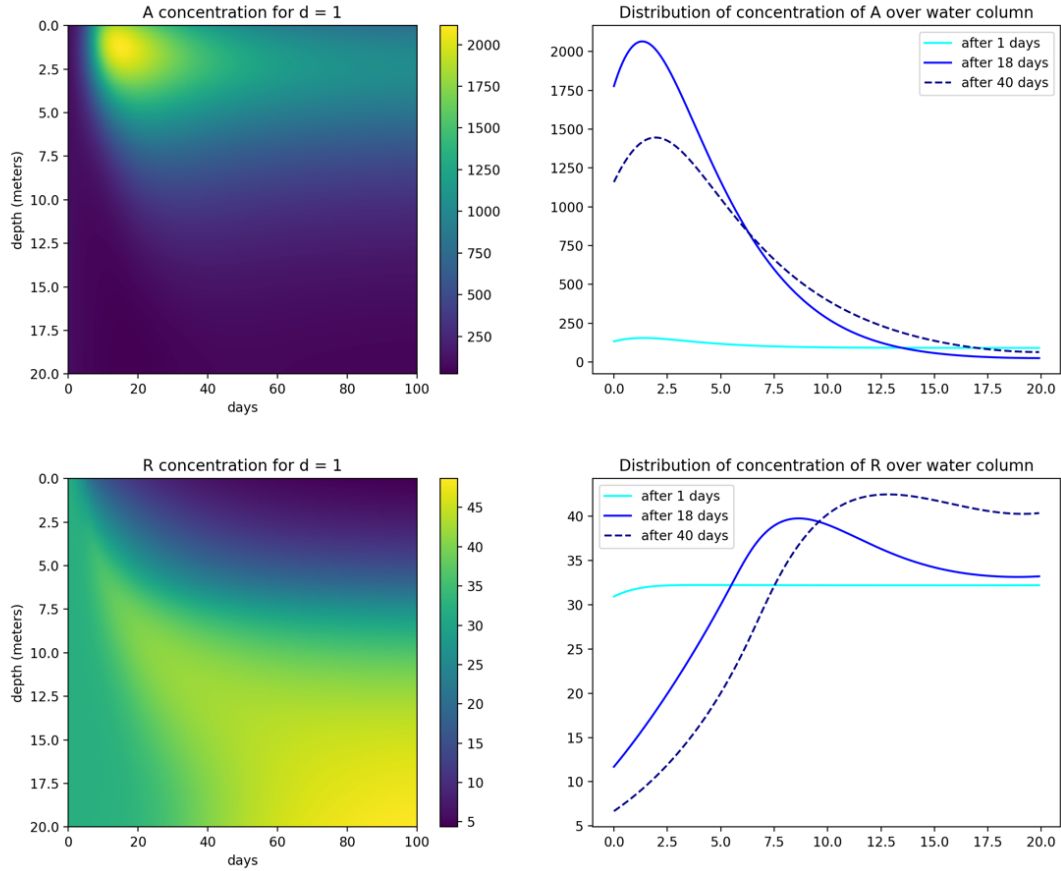


Figure 14: *Heatmaps showing the evolution of phytoplankton and nutrient distributions for the first 100 days.*

Figure 15 zooms in on the moment when light disappears from the surface. The phytoplankton population quickly starts diminishing and it drifts and diffuses downwards. As this happens the nutrient spread becomes more homogeneous.

again

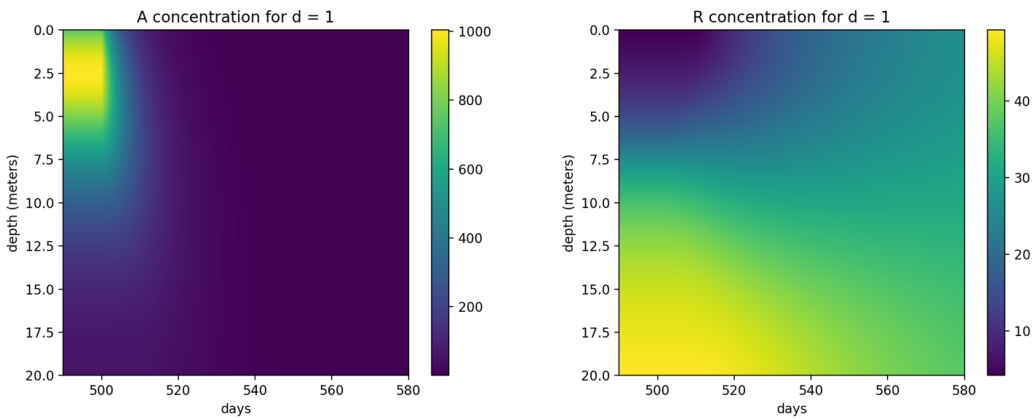


Figure 15: Enlargement of the days when light first disappears
surprising

Figure 16 is interesting because it shows that extremely little algae needs to be present in the system for the population to recover once conditions improve. On day 600 the maximum concentration of A in the water column is around 0.007 but 40 days later the distribution has a peak near 1750. This suggests that the peaked stationary distribution of A is almost globally stable for $A \neq 0$. **mg P m⁻³**

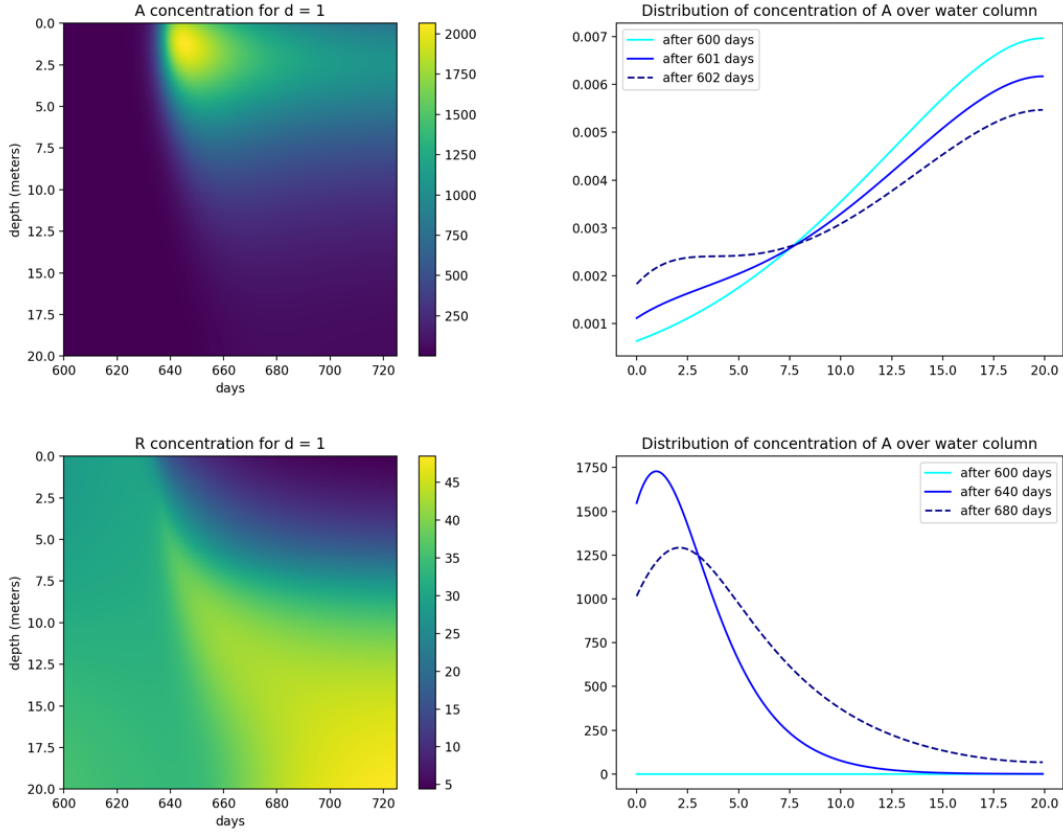


Figure 16: *Enlargement of the days when light returns to normal.*

Population blooms are observed in both figures 14 and 16. These show how, in this model, any small phytoplankton population can lead to a population explosion caused by the availability of nutrients near the surface, which support a large increase in photosynthesis. It is natural to expect an algal population to decrease once light is reduced, as photosynthesis cannot take place, but it is interesting to note that if light conditions return then a population bloom can usually be expected before the algae settles back into its stationary distribution. This is a nice example of the resilient and self-regulating nature of ecosystems.

4 Discussion

4.1 Looking for Bifurcations

One of the aspirations of this project was to find tipping points in the system such that a small change in initial conditions could lead to

References

- [1] Bennett, J., Dolin, R. and Blaser, M. (2015). *Mandell, Douglas, and Bennett's principles and practice of infectious diseases* (8th ed.). Elsevier Saunders, p.3192.
- [2] Bouman, B. (1992). *Linking physical remote sensing models with crop growth simulation models, applied for sugar beet*. International Journal of Remote Sensing, p.2565-2581
- [3] Burden, R. and Faires, J. (2011). *Numerical analysis* (9th ed.). Boston, MA: Brooks/Cole, Cengage Learning, p.348.
- [4] Coons, R. (2018). *Danish researchers look to harness bioluminescent algae to light cities*. [online] Available at: <http://biofuelsdigest.com/nuudigest/2018/05/07/danish-researchers-look-to-harness-bioluminescent-algae-to-light-cities/>
- [5] Encyclopedia Britannica. (2020). *Euphotic zone — oceanography*. [online] Available at: <https://www.britannica.com/science/euphotic-zone>.
- [6] US EPA. (n.d.). *The Effects: Dead Zones and Harmful Algal Blooms — US EPA*. [online] Available at: <https://www.epa.gov/nutrientpollution/effects-dead-zones-and-harmful-algal-blooms>
- [7] Jäger, C., Diehl, S., Matauscheck, C., Klausmeier, C. and Stibor, H. (2008). *Transient Dynamics of Pelagic Producer-Grazer Systems in a Gradient of Nutrients and Mixing Depths*. Ecology, p.1272-1286
- [8] Jäger, C., Diehl, S. and Emans, M. (2010). *Physical Determinants of Phytoplankton Production, Algal Stoichiometry, and Vertical Nutrient Fluxes*. The American Naturalist, p.E91-E104
- [9] Lindsey, R. and Scott, M. (2010). *What are Phytoplankton?*. [online] Available at: <https://earthobservatory.nasa.gov/features/Phytoplankton>
- [10] Lucey, J., Palmer, G., Yeong, K., Edwards, D., Senior, M., Scriven, S., Reynolds, G. and Hill, J. (2017). *Reframing the evidence base for policy-relevance to increase impact: a case study on forest fragmentation in the oil palm sector*. Journal of Applied Ecology, p.731-736.

- [11] McClellan, C., Brereton, T., Dell'Amico, F., Johns, D., Cucknell, A., Patrick, S., Penrose, R., Ridoux, V., Solandt, J., Stephan, E., Votier, S., Williams, R. and Godley, B. (2014). *Understanding the Distribution of Marine Megafauna in the English Channel Region: Identifying Key Habitats for Conservation within the Busiest Seaway on Earth*. PLoS ONE, p.e89720.
- [12] Narwani, A., Lashaway, A., Hietala, D., Savage, P. and Cardinale, B. (2016). *Power of Plankton: Effects of Algal Biodiversity on Biocrude Production and Stability*. Environmental Science Technology, p.13142-13150.
- [13] Petrovskii, S. V., Malchow, H. (2009). *Mathematical Models of Marine Ecosystems*. Oxford, UK: EOLSS
- [14] Rivers-Moore, N., Hughes, D. and de Moor, F. (2008). *A model to predict outbreak periods of the pest blackfly Simulium chutteri Lewis (simuliidae, Diptera) in the Great Fish River, Eastern Cape province, South Africa*. River Research and Applications, p.132-147.
- [15] Sauer, T. (2012). *Numerical analysis* (2nd ed.). Pearson Education, Inc., p.384.
- [16] Scheffer M., van Nes E., Holmgren M. and Hughes T. (2008). *Pulse-Driven Loss of Top-Down Control: The Critical-Rate Hypothesis*. Ecosystems, p. 226–237
- [17] Stoffers, R. (1984). *The Great Tambora Eruption in 1815 and it's Aftermath*. Science, p.1197
- [18] United Nations Population Division (2019). *World Population Prospects 2019 Revision Highlights — United Nations Population Division*. [online] Available at: https://population.un.org/wpp/Publications/Files/WPP2019_Highlights.pdf

In this project an explicit finite difference method was used to approximate the deterministic model provided by Jaeger et al. in \cite{Jaeger 2}. This approximation successfully replicated the results in the depth-turbulence space provided by Jaeger et al. \ref{} and extended the exploration of how changes in light intensity affect a phytoplankton population by generating a number of simulations. It was found that the stationary distributions of these populations are very stable for a fixed set of parameters and that even extremely low initial concentrations of algae are capable of blooming to large populations in a matter of days, provided conditions are favourable. Since phytoplankton form the foundation of life in marine ecosystems \cite{?} this is a comforting reminder of the resilience of nature and its ability to recover from extreme shocks. This model is, however, extremely basic and fundamentally wrong as it fails to account for the innumerable other contributing factors to the survival of phytoplankton species. Any conclusions formed through it need to be verified via much practical experimentation and research. This model does capture some of the fundamental mechanisms by which algal populations survive and can serve as an basic aide to understanding from which more sophisticated model can be built.

A Appendix

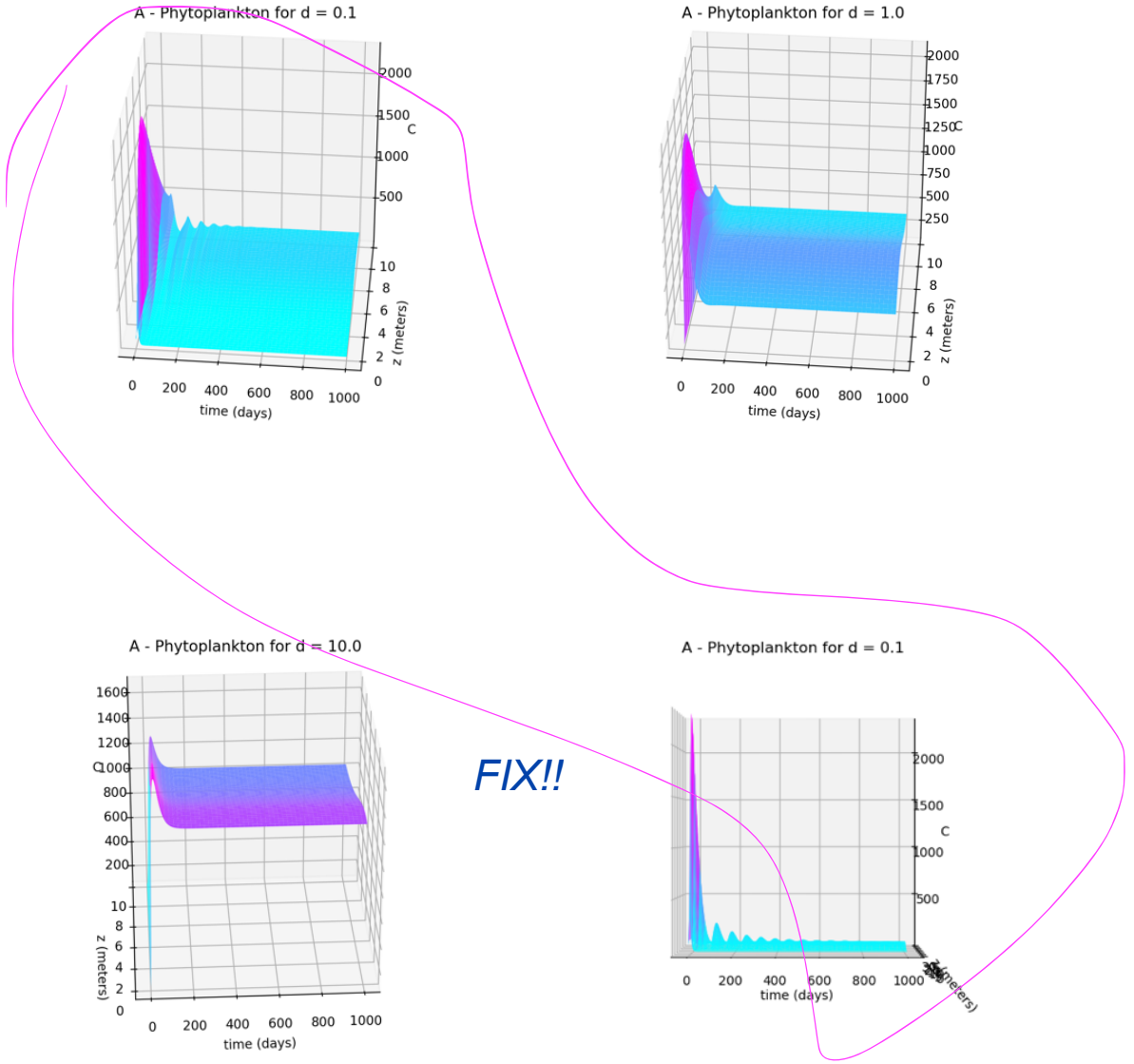


Figure A1: Surface plots for different turbulence and water column depths values. Note that the solution takes longer to settle into a stationary distribution when there are smaller d -values and larger values of z_{max} as in figure (d). Contrast to figure (c) settles into a stationary distribution before $t_{max} = 200$.

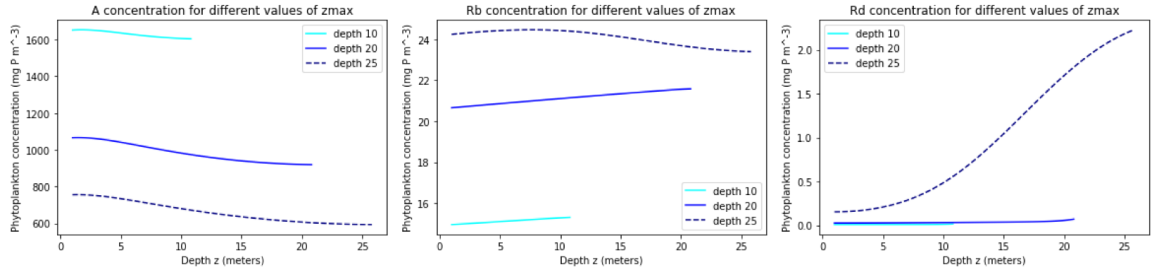


Figure A2: The distributions of phytoplankton, bound and dissolved nutrients for different water column depths when $d=100$. Note that A and R_b are always at a maximum or a minimum at z_{max} and R_d is always at a maximum or a minimum at zero. This is in alignment with the Neumann boundary conditions provided in table 2

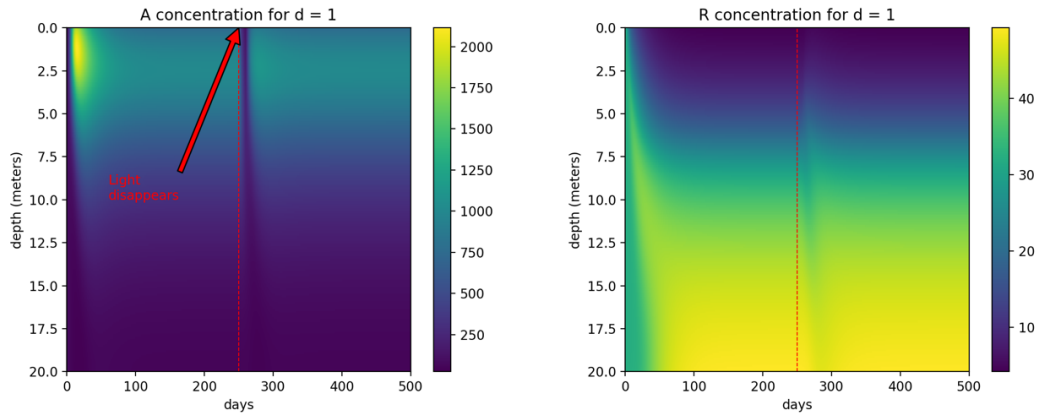


Figure A3: Light disappears for 10 days on the 250th day, $d=1$, $z_{max}=20m$

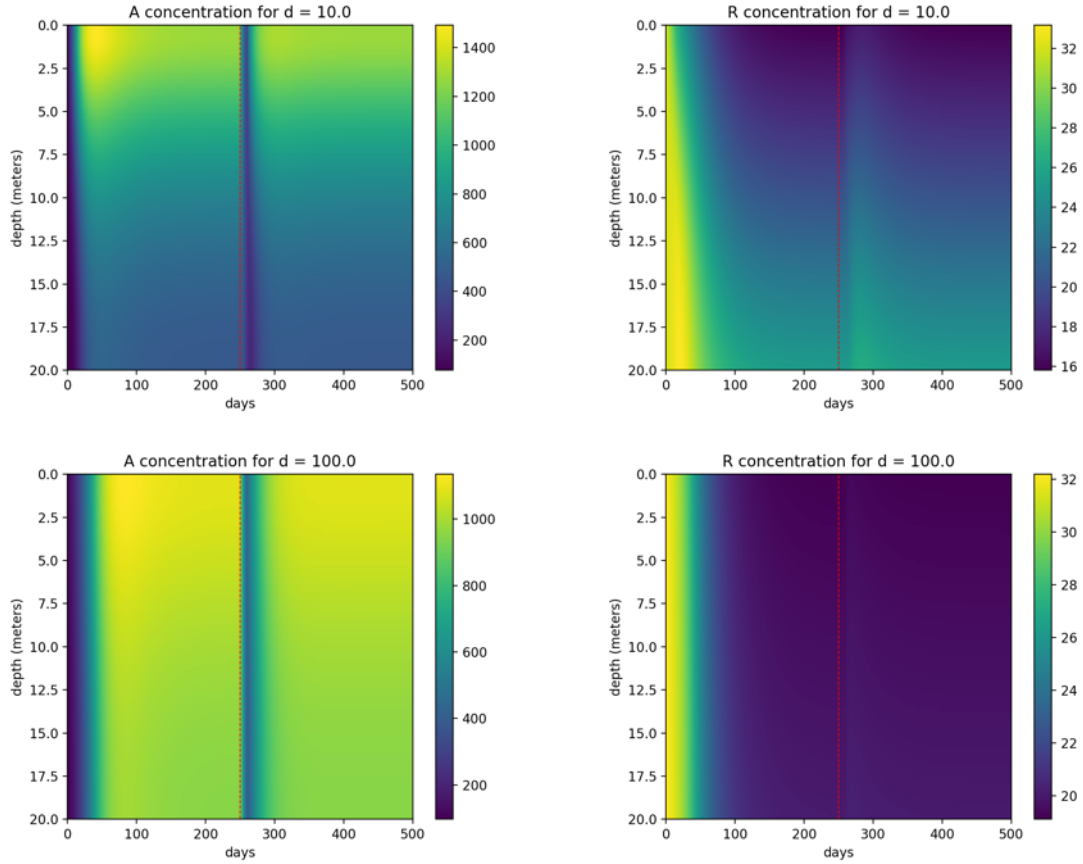


Figure A4: Light disappears for 10 days on the 250th day, for $d=10$ and $d=100$, $z_{max}=20m$. For all values of d studied the system has returned to its stationary distribution within 100 days the light disappearing for 10 days/ of

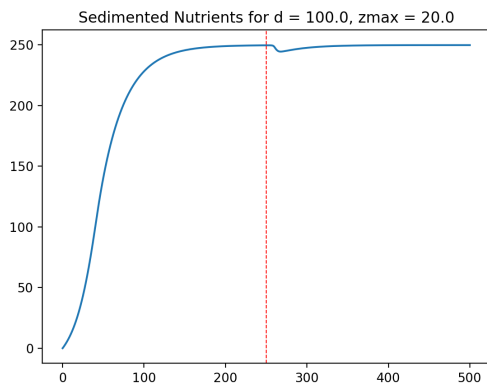


Figure A5: The value of R_s over time for a water column with depth 20 and turbulence $d = 100$. Light shock occurs for 10 days on day 250, which impacts R_s a few days later as the amount of algae and bound nutrients sinking to z_{max} is insufficient to maintain its value of around 250 mg P m^{-2}

add .py module only, put onto cd?